

Ising-Potts models and solid-liquid phase equilibria in binary mixtures

This article has been downloaded from IOPscience. Please scroll down to see the full text article.

1989 J. Phys. A: Math. Gen. 22 4453

(<http://iopscience.iop.org/0305-4470/22/20/021>)

View [the table of contents for this issue](#), or go to the [journal homepage](#) for more

Download details:

IP Address: 129.252.86.83

The article was downloaded on 01/06/2010 at 07:04

Please note that [terms and conditions apply](#).

Ising-Potts models and solid-liquid phase equilibria in binary mixtures

P D McMahon

Department of Chemical Engineering, University of Wisconsin, Madison, WI 53706, USA

Received 1 June 1989

Abstract. An Ising-Potts model is introduced and the Bragg-Williams mean-field method and Monte Carlo simulation are used to study its properties on the FCC lattice. It is shown that for certain values of the parameters in the Hamiltonian the model exhibits phase behaviour that can be interpreted as representing solid-liquid phase equilibria in binary alloy mixtures. The first-order transition properties of the pure six-state Potts model on the FCC lattice are also reported.

1. Introduction

Ising-Potts models combine features of the Ising spin- $\frac{1}{2}$ model and the q -state Potts model. Walker and co-workers have recently applied Ising-Potts models to closed-loop miscibility behaviour in binary liquid mixtures [1-3]. Ferromagnetic Ising interactions in their models lead to binary phase separation at low temperatures. As the temperature is reduced further, the ferromagnetic Potts variables also order. This represents the formation of hydrogen bonds between unlike molecules, and it leads to remixing at the lowest temperatures. In this paper we introduce an Ising-Potts model that can be used to represent solid-liquid equilibria in binary mixtures. In our model the onset of long-range order in the ferromagnetic Potts spins will represent solidification, while ordering of the Ising spins will still represent binary phase separation that can now take place either in the solid or liquid phases. The application of Ising-Potts models to solid-liquid equilibria is particularly appropriate because, like solidification, the ordering of Potts spins is normally a first-order transition. Simple lattice models of the type introduced here may form the basis for needed semiempirical models for solid-liquid equilibria, just as simple Ising-type models have formed the basis for successful liquid mixture excess property models [4]. In § 2 the Ising-Potts model is described, and in § 3 we show, using the Bragg-Williams mean-field method, that this model generates commonly seen solid-liquid equilibrium phase diagrams. We have also carried out Monte Carlo simulations of a simple Ising-Potts model as a check on the mean-field method; the results are reported in § 4, together with the transition properties of the pure six-state Potts model on the FCC lattice, a special case of the Ising-Potts mixture model.

2. The model

We consider the following mixed-spin Ising-Potts model where each site of a regular lattice is occupied by both a two-state Ising spin and a q -state Potts spin. The reduced

Hamiltonian is

$$-\beta\mathcal{H} = \sum_{\langle i,j \rangle} Ks_i s_j + \sum_i Hs_i + \sum_{\langle i,j \rangle} (L_1 \delta_{\sigma_i, \sigma_j} \delta_{s_i, 1} \delta_{s_j, 1} + L_2 \delta_{\sigma_i, \sigma_j} \delta_{s_i, -1} \delta_{s_j, -1} + L_3 \delta_{\sigma_i, \sigma_j} \delta_{s_i, -s_j}) \quad (1)$$

where $s_i = \pm 1$ specifies the Ising spin state at lattice site i , $\sigma_i = 1, \dots, q$ specifies the Potts state at site i , and

$$\delta_{x,y} = \begin{cases} 1 & \text{if } x = y \\ 0 & \text{otherwise.} \end{cases}$$

Only nearest-neighbour and single-site interactions are included in the Hamiltonian. Notice that when $L_1 = L_2 = L_3 = 0$ the model reduces to the $I(\frac{1}{2})$ model, and that when $K = H = 0$ and $L_1 = L_2 = L_3 = L \neq 0$ it reduces to the q -state Potts model. Also, one can show that when $L_2 = L_3 = 0$, the model is equivalent to the lattice-gas (site-diluted) Potts model [5].

We apply the model to solid-liquid phase equilibria by interpreting it in the following manner. If there are N particles in a binary mixture, then let the system volume be divided into N identical cells centred at the vertices of a regular, space-filling lattice. Let each cell be occupied by a single particle—since vacant or multiply occupied cells are not allowed, pressure-density effects are not included in the model. The Ising spin associated with a particular lattice site will specify the identity of the particle occupying the corresponding cell. For a binary mixture s_i will take two values: ± 1 . Nearest-neighbour Ising spins interact in the usual way for mixture models: ferromagnetic interactions ($K > 0$) lead to phase separation at low temperatures, which in the pure Ising model occurs as a second-order transition at a critical point. Thus, we expect that any Ising transition in the Ising-Potts model will correspond to a compositional order-disorder transition in either the solid or liquid phases. Note also that, although one might expect to see several Ising interaction energies in the mixture Hamiltonian, in fact lattice relationships can be used to eliminate all but one Ising parameter, as in the simple Ising model [6].

The foregoing is just the standard correspondence between the Ising ferromagnet and a binary lattice mixture [7]. To complete the correspondence between Ising-Potts models and binary alloys, we associate the Potts spin on each lattice site with the local position of the particle in the cell centred at the site. If two nearest-neighbouring particles are in the same relative positions (i.e. if the Potts spins have the same value), we say that they are at the preferred crystalline separation, as opposed to simply being nearest neighbours in the liquid phase. These 'solidified' particles gain an additional energy of interaction, L , that serves to promote solidification and that determines the melting temperature. This correspondence makes apparent the motivation for including the Potts spins in the model: for large q the pure, zero-field Potts model is known to undergo a first-order transition, and thus, for suitably chosen parameters, we expect the Potts spins in the Ising-Potts model to also exhibit a first-order transition that will represent solidification. The Hamiltonian in equation (1) actually contains three Potts energy parameters: L_1 , L_2 and L_3 . These are related, respectively, to the pure A, pure B and mixture melting temperatures. We expect that $L_1 > 0$, $L_2 > 0$ and $L_3 > 0$ will promote solidification of pure A, pure B and the solid solution, respectively. Finally, since fusion is accompanied by a decrease in order, and the parameter q is a measure of the increased disorder in the liquid state, q can be related to the molar entropy of

fusion. By using the mean-field result for the latent heat of the pure q -state Potts model [8], we find that

$$\Delta S/R = \frac{(q-2)}{q} \ln(q-1).$$

3. The mean-field approximation

Since we are interested in mixtures, it is convenient to switch from magnetic notation to mixture notation. If $s_i = +1$ corresponds to an A molecule and $s_i = -1$ corresponds to a B molecule, the Hamiltonian can be rewritten in terms of compositional variables as

$$-\beta\mathcal{H} = K(N_{AA} + N_{BB} - N_{AB}) + H(N_A - N_B) + \sum_{\sigma=1}^q (L_1 N_{AA} x_{AA\sigma} + L_2 N_{BB} x_{BB\sigma} + L_3 N_{BB} x_{AB\sigma})$$

where N_i is the number of i molecules, N_{ij} is the number of nearest-neighbour pairs of type ij , and $x_{ij\sigma}$ is the fraction of the nearest-neighbour pairs of type ij whose associated Potts spins are both in state σ .

The Bragg-Williams mean-field approximation is equivalent to the following substitutions [9]:

$$N_{ii} = Nz x_i^2/2 \quad N_{ij} = Nz x_i x_j \quad x_{ij\sigma} = x_{i\sigma} x_{j\sigma}$$

where x_i is the mole fraction of species i , $x_{i\sigma}$ is the fraction of molecules of type i that are in Potts state σ , and z is the lattice coordination number. Making these substitutions gives the mean-field Hamiltonian

$$-\beta\mathcal{H}/N = K(2x_A - 1)^2 z/2 + H(2x_A - 1) + \sum_{\sigma=1}^q [L_1 x_A^2 x_{A\sigma}^2 z/2 + L_2 (1 - x_A)^2 x_{B\sigma}^2 z/2 + L_3 x_A (1 - x_A) x_{A\sigma} x_{B\sigma} z].$$

The configurational partition function is

$$Z = \sum_{x_A, \{x_{A\sigma}\}, \{x_{B\sigma}\}} \omega(x_A, \{x_{A\sigma}\}, \{x_{B\sigma}\}) \exp(-\beta\mathcal{H})$$

where ω is the number of configurations possible for given mole and Potts fractions:

$$\omega = \frac{N!}{\prod_{\sigma=1}^q (N x_A x_{A\sigma})! (N x_B x_{B\sigma})!}$$

Approximating $N^{-1} \ln Z$ by the largest term in the summation, we get

$$N^{-1} \ln Z = -\sum_{\sigma}^q [\bar{x}_A \bar{x}_{A\sigma} \ln(\bar{x}_A \bar{x}_{A\sigma}) + \bar{x}_B \bar{x}_{B\sigma} \ln(\bar{x}_B \bar{x}_{B\sigma})] + (Kz/2)(\bar{x}_A - \bar{x}_B)^2 + H(2\bar{x}_A - 1) + \sum_{\sigma=1}^q [(L_1 z/2) \bar{x}_A^2 \bar{x}_{A\sigma}^2 + (L_2 z/2) \bar{x}_B^2 \bar{x}_{B\sigma}^2 + (L_3 z) \bar{x}_A \bar{x}_B \bar{x}_{A\sigma} \bar{x}_{B\sigma}]$$

where the equilibrium values \bar{x}_i and $\bar{x}_{i\sigma}$ correspond to the largest term.

For $L_i > 0$, we look for a ferromagnetic solution for the Potts ordering. Since all q states are equivalent, we can assume that the Potts spins will order in state 1. By analogy with the simple Potts model [8], we can define two Potts order parameters s_A and s_B by

$$x_{A\sigma} = \begin{cases} [1 + (q - 1)s_A]/q & \text{if } \sigma = 1 \\ (1 - s_A)/q & \text{if } \sigma = 2, \dots, q \end{cases}$$

with similar expressions for s_B . Then, the Bragg-Williams expression for the free energy, $f = -N^{-1} \ln Z$, becomes

$$\begin{aligned} f = & \bar{x}_A \ln \bar{x}_A + \bar{x}_B \ln \bar{x}_B - (Kz)(2\bar{x}_A - 1_B)^2 - H(2\bar{x}_A - 1) - L_1 z \bar{x}_A^2 (1 + q_1 \bar{s}_A^2)/2q \\ & - L_2 z \bar{x}_B^2 (1 + q_1 \bar{s}_B^2)/2q - L_3 z \bar{x}_A \bar{x}_B (1 + q_1 \bar{s}_A \bar{s}_B)/q \\ & + \bar{x}_A [(1 + q_1 \bar{s}_A) \ln(1 + q_1 \bar{s}_A) + q_1 (1 - \bar{s}_A) \ln(1 - \bar{s}_A) - q \ln q]/q \\ & + \bar{x}_B [(1 + q_1 \bar{s}_B) \ln(1 + q_1 \bar{s}_B) + q_1 (1 - \bar{s}_B) \ln(1 - \bar{s}_B) - q \ln q]/q \end{aligned}$$

where $q_1 = q - 1$, $\bar{x}_B = 1 - \bar{x}_A$, and the equilibrium values \bar{x}_A , \bar{s}_A , and \bar{s}_B are those that minimise f at a given temperature and field strength. By differentiating and equating the partial derivatives of the free energy to zero, one can obtain the mean-field expressions for the composition and the Potts order parameters. One gets a set of coupled nonlinear equations that must be solved numerically; for convenience, we used a numerical optimisation routine to minimise f directly. The mixture properties and phase diagrams shown below were obtained by minimising f at many different temperatures and field strengths, so as to locate those points in the phase space where the solutions underwent qualitative changes corresponding to phase transitions.

In figures 1-3 we show three types of phase behaviour exhibited by the Ising-Potts model. Other types of behaviour are possible; here the model parameters were chosen so as to represent three specific binary alloy mixtures: Pt-Au, Cu-Ag and Ni-Pb. In each case the full curve shows the mean-field phase diagram while, for comparison, the broken curve shows the smoothed experimental data [10]. In these calculations

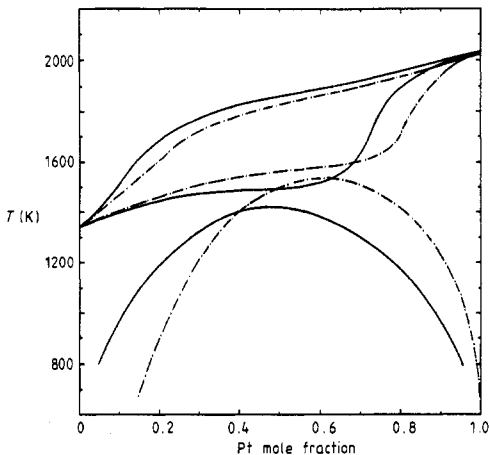


Figure 1. Pt-Au phase diagram (—, BWMF; ---, smoothed data). The Ising-Potts parameters are $K = 127.5 T^{-1}$, $L_1 = 648.7 T^{-1}$, $L_2 = 448.5 T^{-1}$, $L_3 = 600 T^{-1}$.

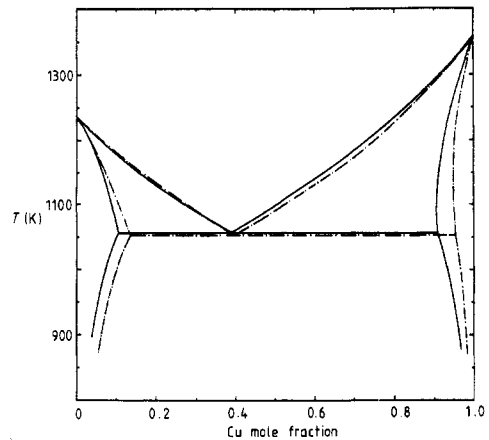


Figure 2. Cu-Ag phase diagram (—, BWMF; ---, smoothed data). The Ising-Potts parameters are $K = 40.0 T^{-1}$, $L_1 = 455.3 T^{-1}$, $L_2 = 414.1 T^{-1}$, $L_3 = 235 T^{-1}$.

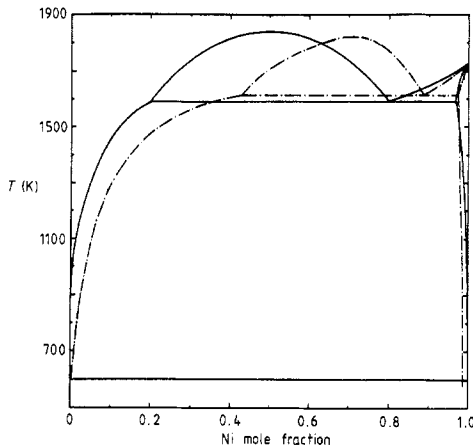


Figure 3. Ni-Pb phase diagram (—, BWMF; ---, smoothed data). The Ising-Potts parameters are $K = 137.5 T^{-1}$, $L_1 = 579.5 T^{-1}$, $L_2 = 201.4 T^{-1}$, $L_3 = 200 T^{-1}$.

all but two of the model parameters were fitted to pure component properties. The parameter q was set by matching the mean-field solution for the entropy of fusion of the pure Potts model to the experimental value for the dimensionless entropy of fusion of the pure metals. $\Delta S/R$ ranges from 0.956 to 1.26 for the six metals considered here [11], implying that $5.5 \leq q \leq 6.9$; for convenience $q = 6$ was chosen. The three binary mixtures and the six pure components all solidify to FCC lattices; accordingly, the lattice coordination number was set to twelve. The remaining pure component parameters, L_1 and L_2 , were chosen to match the pure Potts model mean-field transition temperature [8]

$$L_c = \frac{2(q-1)}{z(q-2)} \ln(q-1)$$

to the experimental melting temperatures of the pure metals [10]. The values are given in figures 1–3. Finally, the two binary parameters, K and L_3 , were adjusted for each binary to fit the experimental phase diagrams.

The Pt–Au binary is the simplest of the three systems and corresponds to a relatively ideal mixture that only shows solid–solid phase separation at low temperatures. Non-idealities are greater in the Cu–Ag mixture and lead to solid–solid immiscibility at higher temperatures and to a binary eutectic. Finally, the Ni–Pb mixture is the most non-ideal, even exhibiting liquid–liquid immiscibility. It also shows two eutectics, although the eutectic point at low temperatures and high Pb compositions cannot be seen on the scale of figure 3. As can be seen in the figures, the Ising–Potts model is capable of showing all three types of behaviour. The fit suffers somewhat from the artificial symmetry imposed by the underlying Ising model but it is qualitatively reasonable for all three systems.

4. Monte Carlo simulations

As a check on the mean-field method, we have carried out Monte Carlo simulations for a simple Ising–Potts model. The simulation was performed at constant temperature and field. Since the field only couples to the Ising spins, in the mixture interpretation

it represents the difference in chemical potentials of the two components. Thus, the simulation yields mixture properties in the semigrand ensemble in which the total number of particles is fixed but the composition can vary [6]. The system simulated consisted of 4000 Ising spins and 4000 six-state Potts spins arranged in a FCC lattice with simple cubic periodic boundary conditions. Some runs were started from ordered initial configurations in which all the Ising spins were of one type and all the Potts spins were in a single state. Other runs were started from the final configurations of earlier runs or from random initial configurations. New configurations were generated by two types of trial move. In the first, an Ising spin was flipped, while keeping the Potts state fixed, and the new configuration was accepted or rejected on the basis of the usual Boltzmann criterion. In the second trial move, a Potts spin was changed to a new state randomly chosen from the $q - 1$ remaining states, and again the move was accepted or rejected using the Boltzmann criterion. A Monte Carlo step (MCS) consisted of a regular sweep over all the spins on the lattice, trying in turn to flip each Ising spin and to change each Potts spin. Thus, each MCS corresponds to 8000 configurations. Runs consisted of 1000–2000 Monte Carlo steps. In the one-phase regions the lattice equilibrated within 100 MCS. Even near phase transitions, 200 MCS was usually sufficient to reach metastable equilibrium, while 1000 MCS was short enough not to sample fluctuations between the coexisting phases. As an example, figure 4 shows the evolution of the running averages of the mole fraction, the configurational energy and the Potts order parameter, for a run at conditions close to a field-induced first-order transition. The averages were computed separately for the first 200 MCS and for the last 800 MCS. Note that by 200 MCS the system has already relaxed from its initial state, a totally ordered configuration. Error estimates for the simulation averages can be determined by the method of Jacucci and Rahman [12, 13]. For the run shown in figure 4, the standard deviations of the mean as a percentage of the mean, $100\sigma(\langle x \rangle)/\langle x \rangle$, are 0.1, 0.1 and 0.3% respectively.

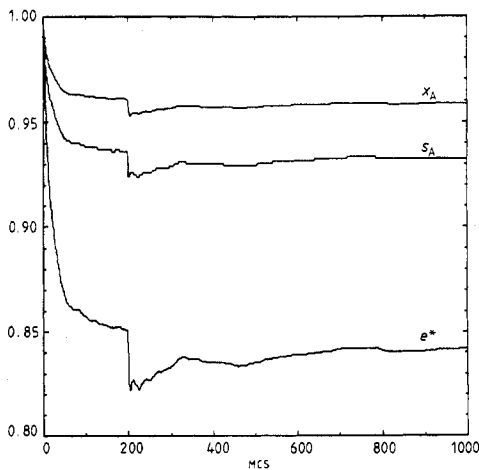


Figure 4. Running averages of the mole fraction (x_A), the relative configurational energy ($e^* = e(\beta, H)/e(\beta, \infty)$), and the Potts order parameter (s_A), during a Monte Carlo simulation of the simple Ising-Potts model at $H = 0.2$, $L_1 = L_2 = 0.4277$, and $L_3 = K = 0$.

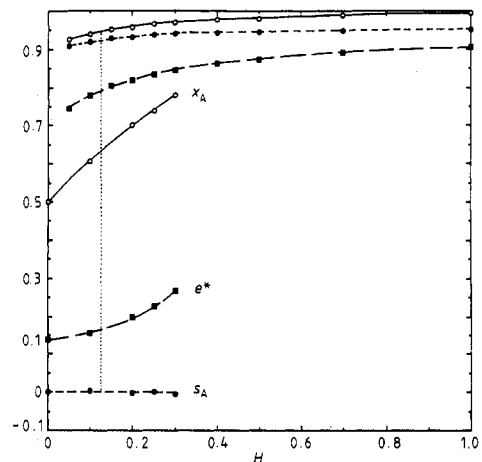


Figure 5. Monte Carlo results for the average mole fraction (x_A), the average relative configurational energy (e^*), and the average Potts order parameter (s_A), as a function of field strength for the simple Ising-Potts model ($L_1 = L_2 = 0.4277$, $L_3 = K = 0$).

Phase transitions were located by checking for hysteresis on changing the initial conditions. This behaviour is seen in figure 5 which shows typical results for the composition, the configurational energy and the Potts order parameter for a series of simulations carried out at constant temperature. At high field the alloy is almost pure solid A, while at low fields it exists as a near-equimolar liquid mixture. The field-induced first-order transition was located more precisely by the method of thermodynamic integration [14]. The effect on the free energy of varying the temperature or the field strength is given by

$$f(H_2, \beta_2) = f(H_1, \beta_1) + \int_{H_1}^{H_2} \langle m \rangle dH + \int_{\beta_1}^{\beta_2} \langle e \rangle d\beta,$$

where $\langle m \rangle$ is the average magnetisation and $\langle e \rangle = \langle -\beta \mathcal{H} / N - Hm \rangle$ is the average reduced configurational energy per particle, both determined from the simulations. As $\beta \rightarrow \infty$ and $H \rightarrow \infty$, the ferromagnetic interaction energies dominate, the lattice becomes totally ordered, and the free energy can be calculated exactly. Alternatively, as $\beta \rightarrow 0$ and $H \rightarrow 0$, entropy dominates, the spins become completely uncorrelated, and the free energy can again be calculated exactly. By carrying out two series of simulations, one for ordered states and the other for disordered states, the free energy can be determined along two approaches to the phase transition by numerically integrating the energy and magnetisation data. The transition can then be located at the intersection of the two branches of the free energy function. We carried out this thermodynamic integration by fitting the simulation data to cubic splines in H or β as appropriate and then using spline quadrature to perform the integrations [15].

Figure 6 shows the Monte Carlo phase diagram for the symmetric Ising-Potts binary mixture ($K = 0$, $L_1 = L_2 > 0$, $L_3 = 0$, and $q = 6$); the points represent the coexisting phases as determined from thermodynamic integration of the Monte Carlo simulation data—the full curves serve as a guide for the eye. Because of the symmetry of this system about $H = 0$ the simulations were only performed for $H \geq 0$. This mixture shows solid-liquid equilibrium, freezing point depression, and also solid-solid partial immiscibility with a binary eutectic. From thermodynamic integration of the simulation

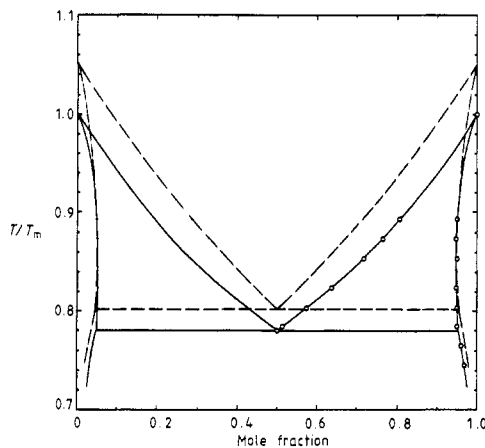


Figure 6. Phase diagram of a symmetric Ising-Potts binary mixture (—, MC results; ---, BWMF) ($L_1 = L_2 > 0$, $L_3 = K = 0$). At the melting point of the pure materials $L_1 = 0.353$.

Table 1. Properties of the simple Ising-Potts model at coexistence as determined by Monte Carlo simulation and thermodynamic integration. The superscripts *s* and *l* denote solid and liquid properties, respectively. The latter are not given for temperatures below the eutectic temperature. At the melting temperature of the pure materials $L_1 = L_2 = 0.3525$ and $K = L_3 = 0$.

T/T_m	H	$-f$	x_A^l	e^l	x_A^s	s_A^s	e^s
1.000	4.000	6.22	1.000	0.559	1.000	0.779	1.48
0.854	0.235	2.79	0.717	0.509	0.949	0.909	1.91
0.824	0.128	2.77	0.635	0.420	0.948	0.925	2.04
0.803	0.063	2.76	0.573	0.392	0.949	0.938	2.15
0.784	0.011	2.77	0.513	0.392	0.951	0.948	2.25
0.765	0.000	2.82	—	—	0.961	0.960	2.40
0.745	0.000	2.88	—	—	0.970	0.968	2.54

Table 2. Size dependence of the Monte Carlo results for the properties of the pure six-state Potts model on the FCC lattice. Also shown are the results of interpolating with N^{-1} to the thermodynamic limit.

N	L	$-f$	e^l	e^s	s
2048	0.3531	2.221	0.5656	1.483	0.7803
4000	0.3525	2.216	0.5591	1.476	0.7793
∞	0.352	2.21	0.552	1.47	0.778

results at zero field we estimate that the reduced eutectic temperature is $T/T_m = 0.78$. Some of the coexistence properties are also given in table 1. For comparison, the mean-field results for this system are also shown in figure 6. Although the mean-field phase diagram is not quantitatively accurate, it is qualitatively correct. This suggests that the mean-field results of the previous section give a reasonable picture of the types of phase diagrams possible in the Ising-Potts model.

In the limit of high field the symmetric Ising-Potts model reduces to a pure six-state Potts model on an FCC lattice; the simulations indicated that at moderate temperatures $H = 4$ was sufficient to completely order the Ising spins. We determined the transition properties of pure Potts model by thermodynamic integration of the high-field data. To check the size dependence of the simulation results, the high-field simulations were repeated for two lattice sizes: $N = 2048$ and $N = 4000$. The results, shown in table 2, indicate that the size dependence is weak for these large values of N . For a first-order transition the properties should extrapolate with N^{-1} to the thermodynamic limit [16, 17]—this gives the following Potts model transition properties: $L = 0.352$, $f = -2.21$, $e^s = 1.47$, $e^l = 0.552$ and $s = 0.778$. Note that f differs from the free energy of the Ising-Potts model at the melting point of pure A. The difference is due to the Ising magnetic field term ($H = 4$), which does not appear in the pure Potts model.

5. Conclusions

In modelling phase equilibria between two or more phases, distinct thermodynamic models are often used for each phase and the equilibrium phase boundaries are

determined by matching chemical potentials in the single-phase models. This is, in fact, the traditional approach to modelling solid-liquid equilibria. However, it is sometimes desirable to have a single Hamiltonian that produces the entire range of phase behaviour. Having a single self-consistent model is important, for example, whenever second-order phase transitions may occur because of the difficulty of matching two independent single-phase models at a critical point or critical end point. The single-model approach to solid-liquid equilibria can take the form of detailed models based on complex intermolecular potentials handled by computer simulations or integral equation theory [18], but such calculations are complex and time consuming. Here we have shown that a simple Ising-Potts lattice model can capture many of the main features of phase equilibrium in binary alloy mixtures. We have also presented Monte Carlo results that suggest that the mean-field method gives qualitatively accurate phase diagrams for these models. Higher-order mean-field methods such as the Bethe or Kikuchi methods, or mean-field renormalisation techniques [19] could be used to obtain greater accuracy in the transition properties.

References

- [1] Walker J S and Vause C A 1980 *Phys. Lett.* **79A** 421
- [2] Walker J S and Vause C A 1983 *J. Chem. Phys.* **79** 2660
- [3] McMahon P D, Glandt E D and Walker J S 1988 *Chem. Eng. Sci.* **43** 2561
- [4] Abrams D and Prausnitz J M 1975 *AIChE J.* **21** 116
- [5] Berker A N, Ostlund S and Putnam F A 1978 *Phys. Rev. B* **17** 3650
- [6] Hill T L 1956 *Statistical Mechanics* (New York: McGraw-Hill) p 290
- [7] Toda M, Kubo R and Saito N 1983 *Statistical Physics I* (New York: Springer) p 121
- [8] Wu F Y 1982 *Rev. Mod. Phys.* **54** 235
- [9] Kubo R 1965 *Statistical Mechanics* (Amsterdam: North-Holland) p 305
- [10] Massalski T B, Murraray J L, Bennett L H and Baker H 1986 *Binary Alloy Phase Diagrams* (Metals Park, Ohio: ASM)
- [11] Weast R C 1980 *CRC Handbook of Chemistry and Physics* 61st edn (Baton Rouge, LA: CRC Press)
- [12] Jacucci G and Rahman A 1984 *Nuovo Cimento D* **4** 341
- [13] Allen M P and Tildesley D J 1987 *Computer Simulation of Liquids* (Oxford: Clarendon) p 192
- [14] Mouritsen O G 1984 *Computer Studies of Phase Transitions and Critical Phenomena* (New York: Springer) p 53
- [15] Press W H, Flannery B P, Teukolsky S A and Vetterling W T 1986 *Numerical Recipes* (Cambridge: Cambridge University Press) p 86
- [16] Binder K and Landau D P 1984 *Phys. Rev. B* **30** 1477
- [17] Challa M S S, Landau D P and Binder K 1986 *Phys. Rev. B* **34** 1841
- [18] Rick S W and Haymet A D J 1989 *J. Chem. Phys.* **90** 1188
- [19] Marques M C 1988 *J. Phys. A: Math. Gen.* **21** 1061